Energy Conversion and Management 87 (2014) 820–831

Contents lists available at ScienceDirect

Energy Conversion and Management

journal homepage: www.elsevier.com/locate/enconman

Energy management strategy based on short-term generation scheduling for a renewable microgrid using a hydrogen storage system

Giorgio Cau [a], Daniele Cocco [a], Mario Petrollese [a,*], Søren Knudsen Kær [b], Christian Milan [b]

[a] Department of Mechanical, Chemical and Materials Engineering, University of Cagliari, Via Marengo, 3 09123 Cagliari, Italy
[b] Department of Energy Technology, Aalborg University, Pontoppidanstræde 101, 9220 Aalborg, Denmark

ARTICLE INFO

Article history:
Received 5 February 2014
Accepted 25 July 2014
Available online 16 August 2014

Keywords:
Stand-alone power system
Hydrogen storage system
Energy management strategy
Photovoltaic systems
Wind turbine

ABSTRACT

This paper presents a novel energy management strategy (EMS) to control an isolated microgrid powered by a photovoltaic array and a wind turbine and equipped with two different energy storage systems: electric batteries and a hydrogen production and storage system. In particular, an optimal scheduling of storage devices is carried out to maximize the benefits of available renewable resources by operating the photovoltaic systems and the wind turbine at their maximum power points and by minimizing the overall utilization costs.

Unlike conventional EMS based on the state-of-charge (SOC) of batteries, the proposed EMS takes into account the uncertainty due to the intermittent nature of renewable resources and electricity demand. In particular, the uncertainties are evaluated with a stochastic approach through the construction of different scenarios with corresponding probabilities. The EMS is defined by minimizing the utilization costs of the energy storage equipment.

The weather conditions recorded in four different weeks between April and December are used as case studies to test the proposed EMS and the results obtained are compared with a conventional EMS based on the state-of-charge of batteries. The results show a reduction of utilization costs of about 15% in comparison to conventional SOC-based EMS and an increase of the average energy storage efficiency.

1. Introduction

According to the IEA [1], today more than one billion people worldwide lack access to electricity. Various options for supplying this electricity need to be considered: these include on-grid, mini-grid, and isolated off-grid configurations. In particular, decentralized options are an important alternative in cases where grid extensions are too expensive. Stand-alone power systems using fossil fuels suffer from the high costs of these fuels, pollution and greenhouse gas emissions, while stand-alone microgrids completely powered by renewable energy sources (RES) can overcome these problems. One of the main drawbacks of using energy conversion systems based on RES, such as photovoltaic systems (PV) and wind turbines (WT), is their discontinuity in energy production, so that an effective energy storage section is required to ensure a continuous electrical energy supply.

Among energy storage systems, batteries are the most common choice for short-term storage. However, for longer-term storage of energy, their application might be inappropriate owing to their low energy storage density and unavoidable self-discharge [2]. Energy storage systems based on hydrogen technologies are one of the most interesting options and have been the subject of many studies and research activities in recent years [2–14]. In hydrogen storage systems, excess electricity can be converted to hydrogen through an electrolyzer (EL) and stored in pressurized tanks. The stored hydrogen can later be used to produce electricity in a fuel cell (FC).

Hydrogen technologies are not yet competitive with large scale energy storage systems, such as pumped hydro storage. However, they have major advantages in stand-alone power systems. Owing to the absence of the electrical grid, stand-alone systems usually rely on internal combustion engines (ICE), which use fossil fuels. The substitution of these fuels with RES, mainly wind turbines and photovoltaic modules, leads to significant reduction of polluting emissions. In this framework, the coupling between hydrogen storage systems and electrical batteries is investigated as a suitable solution in stand-alone power generation plants, which may lead to greater flexibility in following load demand and ensuring both long and short-term energy storage. Depending on the situation, the surplus of electrical energy can be used to charge the electric batteries or the hydrogen tanks. Similarly, the demand can be

* Corresponding author. Tel.: +39 070 6755724; fax: +39 070 6755717.
E-mail address: petrollese@unica.it (M. Petrollese).

http://dx.doi.org/10.1016/j.enconman.2014.07.078
0196-8904/

Nomenclature

Symbols

ρ	probability
A	panel area (m^2)
C	cost (€)
e	percent error
f	objective function
G	solar irradiation (W/m^2)
L	lifetime (h)
N	number of elements
n	molar flow (mol/s)
P	power (W)
p	pressure (Pa)
Q	capacity (Ah)
S	number of scenarios
T	temperature (K)
t	time (h)
U	voltage (V)
V	volume (m^3)
v	wind speed (m/s)
z	height (m)
z_0	roughness height (m)
α	temperature coefficient
η	efficiency
τ	branching time (h)
θ	time horizon (h)

Subscripts

AMB	ambient
B	battery
D	demand
EL	electrolyzer
EX	excess power
FC	fuel cell
G	solar irradiation
H_2	hydrogen
LD	load
MIN	minimum
MAX	maximum
NOM	nominal
PV	photovoltaic panel
REF	reference
s	scenario
UN	undelivered power
w	wind
WT	wind turbine

Acronyms

SOC	state-of-charge
NOCT	nominal operating cell temperature
PEM	Proton Exchange Membrane
EMS	energy management strategy
RES	renewable energy sources
PDF	probability distribution function
O&M	Operation and Management
LHV	lower heating value
MPPT	Maximum Power Point Tracking
GAMS	General Algebraic Modeling System

covered by using the energy stored in one of these two systems. Such highly integrated energy systems require a proper energy management strategy (EMS) to ensure optimal operation of the stand-alone power plant.

The common control parameter used in conventional EMSs is the battery State-of-charge (SOC) [8–11]. Generally, these strategies do not consider the utilization costs and lifetimes of the different devices. A more accurate techno-economic optimization of the overall system requires the inclusion of investment costs, operating costs and lifetimes of the main plant components. In particular, Dufo-Lopez et al. [12] proposed a control strategy based on the minimization of operational costs of stand-alone hybrid systems with hydrogen storage. A different EMS, based on a stand-alone power system that takes into account the utilization cost of the energy storage system, was introduced by Torreglosa et al. [13]. The comparative study carried out by Castañeda et al. [14] highlighted that the EMS based on the minimization of utilization costs leads to a higher utilization of the hydrogen system compared to EMS based on the use of the battery SOC.

The optimal scheduling of the different microgrid components is widely studied in literature. In particular, generation scheduling can be divided into two different problems: Unit Commitment (UC) and Economic Dispatch (ED) [15]. The UC strategy defines the on/off status of generators over a daily or weekly time horizon while respecting system constraints. The ED strategy defines the operating power of the units committed by the UC problem for a shorter time horizon (hourly or in real-time). The determination of the optimal EMS greatly benefits from the inclusion of wind and solar radiation forecasts. In particular, Logenthiran and Srinivasan [16] proposed a three-step algorithm to solve the UC problem for a stand-alone microgrid based on RES and batteries. Zein Alabedin et al. [17] introduced a different methodology based on a multi-scenario stochastic model and the assignment of an additional spinning reserve requirement to take into account forecast uncertainties. In particular, two optimization models to solve the UC problem in a microgrid including RES and batteries operating in grid-connected mode and isolated mode were presented in [17] and several cases studies were examined to investigate the operation of a microgrid. Tuoy et al. [18] examined the benefits of using a stochastic approach instead of a deterministic one to account for the uncertainty of wind in the UC problem for a power generation system with large wind penetration. Possible future wind and load profiles were represented with a scenario tree. The optimal scheduling of a renewable stand-alone microgrid that includes a fuel cell was introduced by Morais et al. [19]. The analysis was carried out with a deterministic approach for a period of one day and the fuel cell was used only as an emergency reserve. A similar analysis was presented by Khodr et al. [20], who simulated a renewable microgrid to propose a method for the optimal management of the next week (672 time steps) in a deterministic environment.

All of these works in the field of EMS are based on a stochastic approach applied to stand-alone microgrids without hydrogen storage systems. This paper proposes a novel EMS that optimizes the scheduling of RES stand-alone power systems that include batteries and hydrogen storage technologies. To demonstrate its capabilities, the proposed EMS is applied to a microgrid powered only by RES and currently under construction at the Concentrating Solar and Hydrogen from Renewable Energy Sources Laboratory as part of the Sardegna Ricerche Renewable Energy Cluster. In particular, a mathematical model to minimize the utilization cost is elaborated. A stochastic approach instead of a deterministic one is chosen and the scenario tree method is used to take into account

the uncertainties of both forecast weather and load profiles. In this paper the proposed EMS is presented and compared with a conventional SOC-based EMS with reference to a stand-alone micro-grid powered by a photovoltaic array and a wind turbine integrated with electric batteries and a hydrogen storage system.

2. Modeling of the hybrid system

The purpose of this study is to develop an optimization model for load generation scheduling of a hybrid micro-grid taking into account the uncertainty of both resource availability and energy demand. The focus is on a stand-alone hybrid microgrid completely powered by photovoltaic systems and wind turbines. In particular, the system configuration considered here refers to the microgrid of the Hydrogen from Renewable Energy Sources Laboratory. The purpose of this laboratory is the implementation, testing and demonstration of technologies related to the production, storage and use of hydrogen from renewable energy sources. Currently, laboratory activities include the development of prototype plants, the characterization and integration of individual components and the overall power generation system, as well as the identification of optimum design criteria in accordance with component specifications and the electricity demand curve. For this reason, the laboratory includes a microgrid powered exclusively by RES to satisfy the energy demand of the laboratory itself. Fig. 1 shows the configuration of the stand-alone hybrid system. In particular, the hydrogen storage system includes a PEM electrolyzer, four independent tanks having an overall storage capacity of 55 N m^3 (13.8 bar and 1 m^3 each) and a 5 kW PEM fuel cell. To study and compare different storage options, a bank of 32 lead-acid batteries is also included. Table 1 shows the main characteristics of the microgrid devices whereas Table 2 shows their costs and expected lifetimes.

To enable the EMS to predict the performance of the system, a simple simulation model of each device is introduced together with the assessment of respective utilization costs. In the following subchapters, the simulation models for each component are described in detail. Despite the lower accuracy, the adoption of simple simulation models is essential to reduce the computational time and to allow a fast running of the EMS during the operating phase of the microgrid. On the contrary, more accurate simulation models should be used for the design of the power generation system as well as during the verification phase of the EMS performance. For this reason, the simulation models used here for evaluating the expected performance of the microgrid as a result of the generation scheduling defined by the EMS. The latter simulation models were already presented in a previous work [26] and just their basic features are reported in this paper.

2.1. Photovoltaic system

It is assumed that the PV system always operates at its maximum power point and therefore its operation is independent of the EMS. At a given irradiation condition and module temperature, the working voltage of the PV is adjusted by the MPPT (Maximum Power Point Tracking) control system to maximize the power output of the array. The following relation is used to describe the power output P_{PV} of the PV system:

$$P_{PV} = G \cdot A_{PV} \cdot N_{PV} \cdot \eta_{PV} \tag{1}$$

where G is global sun irradiance (W/m^2), A_{PV} the panel area (m^2), N_{PV} the total number of panels. The efficiency of the solar panel η_{PV} is expressed as a function of irradiance G and ambient temperature T_{AMB} as follows:

$$\eta_{PV} = \eta_{PV,REF}\left[1 - \alpha\left(T_{AMB} + G\frac{NOCT - 20}{800} - T_{REF}\right)\right] \tag{2}$$

where $\eta_{PV,REF}$ is the efficiency of the panel under reference conditions (1000 W/m^2 of solar irradiation and 25 °C of cell temperature), α is the temperature coefficient (1/K), $NOCT$ is the nominal operating cell temperature and T_{REF} is the reference module temperature (25 °C). All of these parameters are provided by the panel manufacturer [21].

2.2. Wind turbine

Similar to the PV system, the power produced by the wind turbine is independent of the EMS. The power curve is provided by the manufacturer and is depicted in Fig. 2 as a function of wind speed at hub height [22]. Wind speed is measured at the anemometer height (z_{AN}) and therefore a wind shear is modeled to calculate the wind speed at the turbine hub height (z_{WT}). Wind shear is a function of both altitude and roughness of the ground. The relation

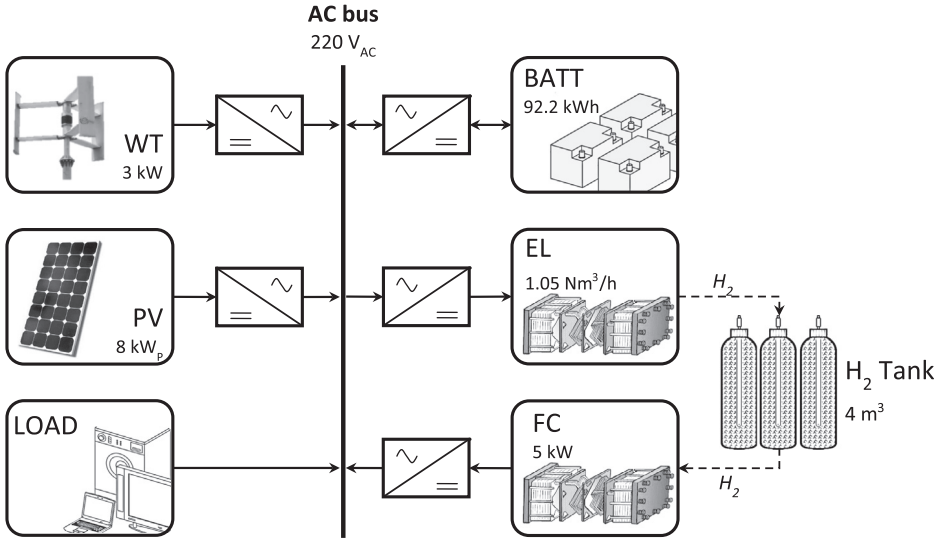

Fig. 1. Configuration of the stand-alone hybrid systems.

Table 1
Main components and characteristics of the microgrid.

Photovoltaic system		Hydrogen storage system	
Panel peak power	0.225 kW	*Electrolyzer*	
Nominal efficiency, $\eta_{PV,REF}$	18.1%	Nominal power	6 kW
Number of panels, N_{PV}	36	H_2 production rate:	1.05 Nm^3/h
Panel area, A_{PV}	1.244 m^2	Delivery pressure	13.8 bar
Solar cell material	Monocrystalline silicon	Electrolyte	PEM
Temperature coefficient, α		*Fuel cell*	
NOCT	−0.38%/K	Nominal power	5 kW
	45 °C	H_2 rated consumption	3.90 Nm^3/h
		Electrolyte	PEM
Wind turbine		**Batteries**	
Rated power @ 14 m/s	3 kW	Nominal voltage, U_B	12 V
Configuration	3 Blades, vertical axis	Rated capacity (C20), Q_B	240 Ah
Rotor diameter	4	Number of batteries, N_B	32
Hub height, z_{WT}	5.8 m	Batteries per string	4
Anemometer height, z_{AN}	2 m	Type	Lead-acid

Table 2
Costs and estimated lifetime for storage devices.

	Batteries	Electrolyzer	Fuel cell
Investment cost	400 €/battery	75,000 €	28,000 €
Estimated lifetime	1300 cycles (DOD = 30%)	30,000 h	30,000 h
O&M cost	–	0.2 €/h	0.2 €/h

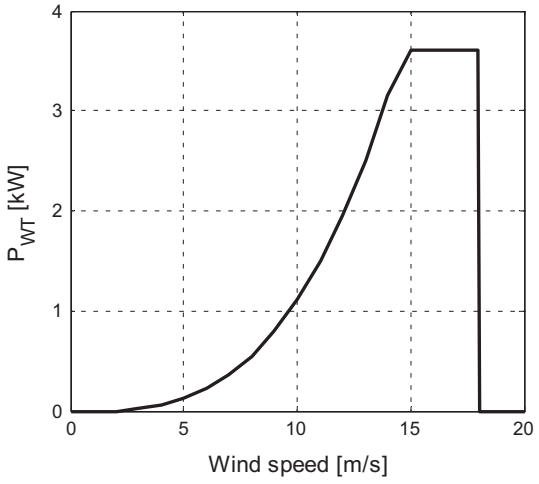

Fig. 2. Wind turbine power curve (Ropatec Simply [17]).

used to calculate wind speed at hub height (v_{WT}) as a function of wind speed measured by the anemometer (v_{AN}) is:

$$v_{WT} = v_{AN} \cdot \ln\left(\frac{z_{WT}}{z_0}\right) \Big/ \ln\left(\frac{z_{AN}}{z_0}\right) \quad (3)$$

z_0 being the surface roughness assumed here as 0.0025 m. Based on wind speed at hub height, the power output of the wind turbine is calculated from the manufacturer's power curve.

2.3. Batteries

The use of batteries to compensate for the differences between energy production and energy demand is the most common solution in microgrid projects involving RES. The addition of a hydrogen storage system leads to a different managing of batteries to maximize their efficiency and lifetime. The available energy content of an electric battery is commonly measured through the so-called "state of charge" (SOC). The latter is the ratio between

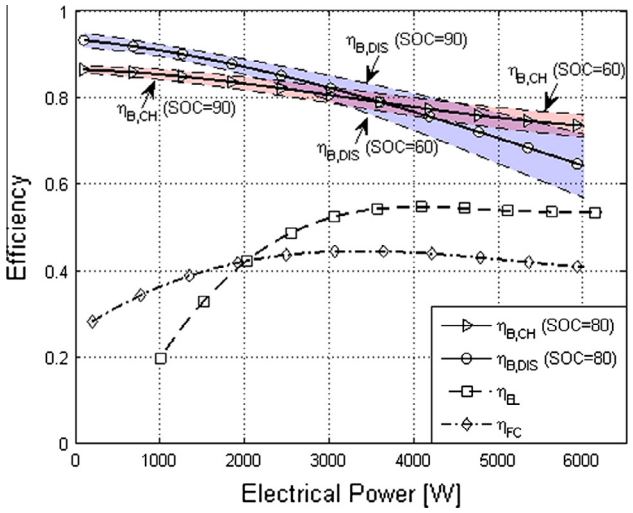

Fig. 3. Batteries, electrolyzer and fuel cell efficiency as a function of power and SOC (the efficiency of batteries varies within the shaded area according the SOC).

the stored energy and its nominal storage capacity and is calculated by monitoring the charging ($P_{B,CH}$) and discharging power ($P_{B,DIS}$) over time:

$$SOC(t) = SOC(t-1) + \frac{\left(P_{B,CH} \cdot \eta_{B,CH} - P_{B,DIS}/\eta_{B,DIS}\right)\Delta t}{N_B U_B Q_B} \quad (4)$$

where $\eta_{B,CH}$ and $\eta_{B,DIS}$ are the battery efficiencies during charge and discharge processes respectively, Δt is the applied time step (h), N_B is the number of batteries, Q_B is the battery nominal capacity (Ah) and U_B is the battery nominal voltage (V). Battery efficiency is expressed in function of the SOC and the input/output power and is calculated in accordance with [23]. The inverter/rectifier has the task of controlling and managing the battery bank. The manufacturer provided the inverter efficiency curve as a function of power [24]. The battery efficiency including inverter losses is shown in Fig. 3 as a function of power and SOC (shaded area).

2.4. Hydrogen storage system

The use of hydrogen storage systems, alone or in addition to batteries, has been the subject of several studies and research activities in recent years. In hydrogen storage systems, an electrolyzer produces hydrogen when the power delivered by RES is higher than demand. Applying Faraday's law, the hydrogen molar

flow of the electrolyzer ($n_{H_2,EL}$) can be expressed as a function of the supplied electric power (P_{EL}):

$$n_{H_2,EL} = \frac{\eta_{EL} P_{EL}}{LHV_{H_2}} \tag{5}$$

where LHV_{H2} is the lower heating value of hydrogen (240 MJ/kmol) and η_{EL} is electrolyzer efficiency, which takes into account electrochemical, thermodynamic and ancillary losses.

The hydrogen can be used to produce electrical energy by means of a fuel cell during peaking periods. Hydrogen consumption of the fuel cell ($n_{H_2,FC}$) is directly related to its power output (P_{FC}) through the following relationship:

$$n_{H_2,FC} = \frac{P_{FC}}{\eta_{FC} LHV_{H_2}} \tag{6}$$

where η_{FC} is fuel cell efficiency, which takes into account electrochemical, thermodynamic and ancillary losses. In accordance with [25,26], both η_{EL} and η_{FC} are expressed in function of input/output power, as shown in Fig. 3.

An important control variable of a hydrogen storage system is the hydrogen tank pressure $p_{H2}(t)$ at a certain time t. Tank pressure is a measure of the hydrogen content of the vessels and can be expressed in function of the produced ($n_{H2,EL}$) and consumed hydrogen molar flows ($n_{H2,FC}$) as well as the pressure at the previous time step $p_{H2}(t-1)$ as follows:

$$p_{H_2}(t) = p_{H_2}(t-1) + \frac{\mathcal{R} T_{H_2}}{V_{H_2}} (n_{H_2,EL} - n_{H_2,FC}) \tag{7}$$

where $\mathcal{R}$ is the gas constant, T_{H_2} is the mean temperature inside the vessel (assumed here constant and equal to 313 K) and V_{H_2} is the overall tank volume (4 m^3 in this study). It is worth noting that the maximum hydrogen pressure is relatively low (13.8 bar) and this is why the ideal gas law is used.

2.5. Excess and undelivered power

Load shedding and power curtailment are often required to maintain the power balance of the system. If demand exceeds the capacity of renewable generators and the storage system is unable to cover this deficit, load shedding is needed to preserve the power balance. Vice versa, if the entire demand can be supplied by the renewable generators and storage systems are fully charged, any excess of renewable energy cannot be stored and a reduction of the power produced by the generators is necessary. Both load shedding and power curtailment options are introduced in the power balance through two variables: undelivered power (P_{UN}) and excess power (P_{EX}) respectively.

3. Problem formulation

Since the system is solely powered by non-controllable renewable sources, PV and WT are operated at all times at their maximum power point. Therefore, power output is directly a function of solar radiation and wind speed respectively. In particular, starting from the forecast of solar radiation, ambient temperature and wind speed conditions, the expected power produced by the photovoltaic system and wind turbine were calculated for each time step Δt of the overall time period θ. For given values of the forecasted load demand, the purpose of the EMS is to determine the optimal operation of storage devices (batteries, electrolyzer, fuel cell) to give the minimum operating cost of the overall microgrid. According to the scheduling determined by the EMS, the power values of each device (P_i) are linked with binary variables (Y_i) that determine the status of the device, as better explained in the following.

3.1. Utilization costs

When excess power produced by PV and WT generators needs to be stored, the EMS allows assessment of the most convenient storage system. In particular, the EMS calculates and compares the utilization costs of batteries and the hydrogen storage system for cycling the energy corresponding to available power P during a time step Δt. Because of the absence of fuel costs, utilization cost C takes into account only depreciation and replacement costs C_{IN} and operating and maintenance cost $C_{O\&M}$ for each device used:

$$C = \frac{1}{\eta} \sum\nolimits_i \left(\frac{C_{IN,i}}{L_i} + C_{O\&M,i} \right) \tag{8}$$

where L_i is the lifetime of the i-th device and η is the roundtrip efficiency. The latter has been included in Eq. (8) to take into account the different energy losses inside the storage systems and to carry out the comparison referring to the same output and not input energy.

Starting from Eq. (8) and according to [12], the battery utilization costs $C_{B,CH}$ during charging are calculated as:

$$C_{B,CH} = \frac{C_{B,IN}/L_{B,CH} + C_{O\&M,B}}{\eta_{B,CH} \eta_{B,DIS}} \tag{9}$$

where $C_{B,IN}$ is the capital cost of the battery bank (€) and $L_{B,CH}$ (h) is the battery lifetime evaluated during charging while the product of the battery efficiencies during charging and discharging processes gives the battery roundtrip efficiency. The batteries' O&M costs $C_{O\&M,B}$ are of minor importance and are neglected in this study.

The lifetime $L_{B,CH}$ in terms of hours is difficult to know, while it is more significant to refer to the equivalent full charge/discharge cycles N_{CYCLES}

$$L_{B,CH} = \frac{N_B U_B Q_B}{P_{B,CH}} N_{CYCLES} \tag{10}$$

In Eq. (10), the ratio of the cycled energy and its nominal capacity gives the battery operation time in terms of equivalent full cycles.

Similar to battery utilization costs during charging, the hydrogen storage utilization costs refer to the costs of producing hydrogen through the electrolyzer and using it for fuelling the fuel cell:

$$C_{H2,CH} = \frac{(C_{EL,IN}/L_{EL} + C_{O\&M,EL}) + (C_{FC,IN}/L_{FC} + C_{O\&M,FC}) \cdot \Delta t_{FC}/\Delta t}{\eta_{EL} \cdot \eta_{FC}} \tag{11}$$

where $C_{EL,IN}$ and $C_{FC,IN}$ are electrolyzer and fuel cell acquisition costs, L_{EL} and L_{FC} electrolyzer and the fuel cell lifetimes, $C_{O\&M,EL}$ and $C_{O\&M,FC}$ the O&M costs of the electrolyzer and the fuel cell, η_{EL} and η_{FC} are the electrolyzer and fuel cell efficiencies and $\Delta t_{FC}/\Delta t$ is the operation time of the fuel cell. Unlike the assumption of [12], the fuel cell operation time is different from the electrolyzer operation time. The operation time $\Delta t_{FC}/\Delta t$ is calculated assuming that the fuel cell operates at its nominal power $P_{NOM,FC}$ and uses all the hydrogen produced by the electrolyzer during the time step Δt:

$$\Delta t_{FC}/\Delta t = \eta_{EL} \cdot \eta_{FC} \cdot \frac{P_{H2,CH}}{P_{NOM,FC}} \tag{12}$$

Similarly, if the user's energy demand has to be provided by the storage system, the EMS calculates the cost of supplying the energy with the batteries or the fuel cell.

If the energy demand has to be provided by the storage system, battery utilization costs during the discharge phase are equal to the average cost of supplying a certain power $P_{B,DIS}$ with the batteries for a time step Δt and is calculated as:

$$C_{B,DIS} = C_{B,IN}/L_{B,DIS} + C_{O\&M,B} \tag{13}$$

where $L_{B,DIS}$ (h) is the battery lifetime evaluated in a discharging step and defined as:

$$L_{B,DIS} = \frac{N_B U_B Q_B}{P_{B,DIS}/\eta_{B,DIS}} N_{CYCLES} \quad (14)$$

If the energy demand has to be provided by the storage system, the utilization cost of supplying the energy with the fuel cell C_{FC} is the average cost of supplying the power P_{FC} for a time step Δt:

$$C_{FC} = C_{FC,IN}/L_{FC} + C_{O\&M,FC} \quad (15)$$

Finally, to avoid load shedding and power curtailment as much as possible, virtual costs were associated with undelivered power (C_{UN}) and excess power (C_{EX}). In particular, the specific costs for undelivered and excess power were set to 0.005 €/W h.

3.2. Scenario tree

The scenario tree approach was adopted to introduce uncertainties into the methodology, since weather data can be forecast only within a very limited time frame and is always subject to deviations. Similarly, another system variable that cannot be directly controlled is the actual energy demand of the microgrid, which depends on many factors (weather conditions, occupants' behavior, etc.). To deal with these uncertainties in energy consumption and electricity production from PV and WT, a stochastic approach was chosen. Tuohy et al. [18] compared stochastic and deterministic methods for scheduling energy systems with high wind penetrations and state that stochastic optimization models perform better in terms of operational costs and precision. In this work, a scenario analysis is applied as a special stochastic method.

Forecasting errors in load profiles, wind speed and solar radiation are usually represented through a probability distribution function (PDF) curve as shown in Fig. 4. The generation of the different scenarios is carried out through a discretization of the PDF curve of the forecasting errors by a set of finite states (solid dots in Fig. 4) such that a probability is assigned to each state [17,28]. In this way, by coupling the error value of the ith state (e^i)with its corresponding probability (ρ^i), it is possible to define discrete probability distribution sets for load demand (δ_D), wind speed (δ_W) and solar radiation (δ_G) in accordance with [17]:

$$\delta_D = \{(e_D^1, \rho_D^1), (e_D^2, \rho_D^2), \ldots, (e_D^n, \rho_D^n), \} \quad (16)$$

$$\delta_W = \{(e_W^1, \rho_W^1), (e_W^2, \rho_W^2), \ldots, (e_W^m, \rho_W^m), \} \quad (17)$$

$$\delta_G = \{(e_G^1, \rho_G^1), (e_G^2, \rho_G^2), \ldots, (e_G^q, \rho_G^q), \} \quad (18)$$

where n, m and q are the number of states in the discrete set of load, wind speed and solar radiation forecasting errors. A set of scenarios can be created from the discrete sets δ_D, δ_W and δ_G to take into account possible deviations from the load, wind speed and solar radiation forecasting values. The product of the number of states n, m and q is equal to the total number of scenarios (S), whereas the probability for each scenario (ρ) is equal to the product of the probabilities of the states corresponding to that scenario.

As described in [27], the usual approach for a scenario analysis is to model the set of S independent scenarios to find the best one. However, this approach is very calculation intensive, since in many cases a large number of scenarios have to be considered. Moreover, the calculations must be continuously replicated when the new forecasts are available. To reduce the number of decision variables Pallottino et al. [27] used a so-called scenario tree approach, which aggregates into a single bundle the set of scenarios sharing a common portion of data. In this way, the common portions of the S independent scenarios are aggregated into bundles by producing a tree structure, as shown in Fig. 5. The main concepts behind the aggregation process of the scenario tree are the branching time and the stage. The branching time τ is the time in which the scenarios begin to differ, while a stage is the time period between two branching times. Each dot of Fig. 5 represents the state of the microgrid during a time step Δt. Up to the first branching time, that is during stage 0, all decisions for the different scenarios are the same. After the first branching time, stage 1 begins with different decisions for each scenario, and so on through the following stages. During stage 0 of the scenario tree the state of the microgrid is common to all the scenarios. The main rules adopted to organize the scenario tree are described in [27].

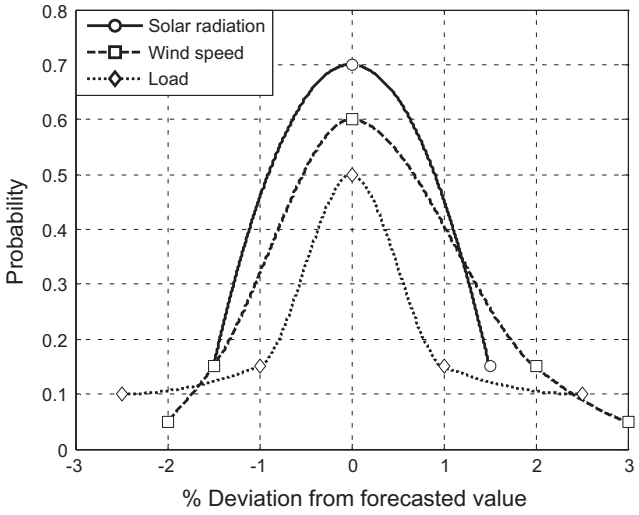

Fig. 4. Discretized probability distribution functions of the load, wind speed, and solar radiation forecasting errors.

Rolling planning is used to update data and permit a continuous revision of the results. Starting from the current conditions, the storage systems are scheduled until the first branching time. This schedule is updated for any given rolling time.

3.3. Mathematical model

The purpose of the EMS based on short-term generation scheduling is to determine for each time step the status of the overall microgrid giving the minimum operating costs. For this reason, the objective function (f) is formulated in such a way as to minimize the sum of the utilization cost of devices (batteries,

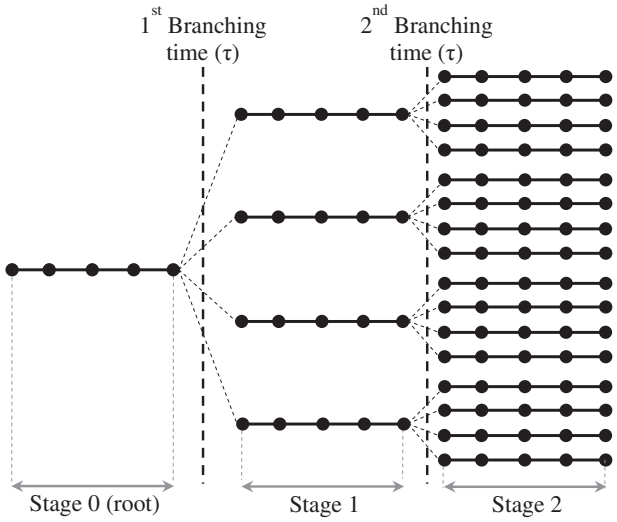

Fig. 5. Scenario tree structure.

electrolyzer and fuel cell) included in the two energy storage systems during the charging/discharging processes and costs related to excess and undelivered power:

$$f = \min \sum_{s=1}^{S} \rho(s) \sum_{t=1}^{\theta} [C_{B,CH}(s,t) + C_{B,DIS}(s,t) + C_{H2,CH}(s,t) + C_{FC}(s,t) + C_{EX}(s,t) + C_{UN}(s,t)] \quad (19)$$

The minimization problem is subject to the following constraints:

(1) Energy balance equation:

$$P_{PV}(t) + P_{WT}(t) + P_{B,DIS}(t) \cdot Y_{B,DIS} + P_{FC}(t) \cdot Y_{FC} + P_{UN}(t) = P_{LD}(t) + P_{B,CH}(t) \cdot Y_{B,CH} + P_{EL}(t) \cdot Y_{EL} + P_{EX}(t) \quad (20)$$

where binary variables (Y_i) determine the status of the device (1 = on, 0 = off). The overall input power in the microgrid has to be equal to the overall output power, whatever the time step and scenario.

(2) Unit generation limits:

$$P_{B,CH}(t), P_{B,DIS}(t) \leqslant P_{B,MAX} \quad (21)$$

$$P_{EL,MIN} \leqslant P_{EL}(t) \leqslant P_{EL,MAX} \quad (22)$$

$$P_{FC,MIN} \leqslant P_{FC}(t) \leqslant P_{FC,MAX} \quad (23)$$

For batteries, maximum charging and discharging power ($P_{B,MAX}$) was introduced since efficiency decreases considerably for high power flows. For the same reason, a limit on maximum power was introduced for electrolyzer ($P_{EL,MAX}$) and fuel cell ($P_{FC,MAX}$). In addition, although the electrolytic cells can efficiently operate even at low power levels, a significant increase in ancillary losses occurs at low values of power with a decrease in efficiency. Therefore, a limit on the minimum power of electrolyzer and fuel cell ($P_{EL,MIN}$ and $P_{FC,MIN}$) was also imposed.

(3) Storage limits:

$$SOC_{MIN} \leqslant SOC(t) \leqslant SOC_{MAX} \quad (24)$$

$$p_{H_2,MIN} \leqslant p_{H2}(t) \leqslant p_{H_2,MAX} \quad (25)$$

The batteries usually have a minimum SOC (SOC_{MIN}) recommended by the manufacturer below which they should not operate. The minimum SOC value greatly affects battery lifetime because a deep discharge of the batteries causes a significant decrease in the number of cycles before replacement. The maximum SOC (SOC_{MAX}) is usually reached when batteries are fully charged (100% of the SOC).

Since a compressor is not included in the hydrogen storage section, the maximum pressure of the hydrogen tanks ($p_{H_2,MAX}$) corresponds to the hydrogen delivery pressure of the electrolyzer. In addition, a constraint on fuel cell supply pressure is imposed by the manufacturer. This limit therefore corresponds to the minimum pressure achievable in the hydrogen tanks ($p_{H_2,MIN}$).

(4) Congruity constraint:

$$Y_{B,EL,FC}(t < \tau, s_1) = Y_{B,EL,FC}(t < \tau, s_2) \ \forall s_1, s_2 \in s \quad (26)$$

This constraint requires that the binary variables determining the status of batteries, electrolyzer and fuel cell in each scenario of the same bundle are identical up to the following branching time.

The formulated problem involves continuous and binary variables. The nonlinear efficiency curves of batteries, electrolyzer and fuel cells introduce a nonlinear behavior of utilization costs (Eq. (9), (11) and (13)) as well as of SOC (Eq. (4)) and p_{H2} (Eq. (7)). However, through a piecewise linear approximation [29] it is possible to solve the problem as a mixed-integer linear programming (MIP) problem using Gurobi [30].

4. Case study

4.1. Input data

The capabilities of the optimization approach presented were evaluated with reference to the microgrid configuration of the aforementioned Hydrogen from Renewable Energy Sources Laboratory. The analysis was carried out with reference to four different case studies: a week in August (summer case), a week in October (autumn case), a week in December (winter case) and a week in April (spring case). Time step Δt and branching time τ were set equal to 0.25 h and 6 h respectively and a time horizon of 4 days was set to take into account the possible evolution of load and weather. All these parameters were subjected to a sensitivity analysis and were optimized for the physical problem under consideration. Forecast data of solar radiation, wind speed and direction as well as ambient temperature with a sampling time of 1 h were provided by accredited institutions [31,32] and refer to the weather station in the ENEA Casaccia Research Centre (near Rome). A rolling time of one hour was imposed and weather forecast data were updated every 24 h. Starting from the forecast of solar radiation and wind speed conditions, the expected power produced by the photovoltaic system and wind turbine were calculated. This expected power represents the main scenario, but other scenarios were introduced with a corresponding probability to take forecasting errors into account. Concerning the load profile, since measured data were not available, according to the information available on laboratory activities, a variable load with an 8 h peak period centered at noon was assumed. In particular, a peak load of 3200 W and a base load of 800 W for the remaining hours were assumed with an overall daily energy demand of 38.4 kW h. As demonstrated in a previous paper [34], the latter load values maximize the energy supplied to the microgrid and ensure that the demand is covered throughout the year.

Data for the PDF of forecasting errors in load profiles, wind speed and solar radiation were extrapolated from [28]. The PDFs for the load profile and wind speed were discretized into 5 states whereas only 3 states were used to discretize the PDF curve of solar radiation, as shown in Fig. 4. Consequently, a total of 75 scenarios were obtained. To decrease computational complexity and running time, the total number of scenarios was reduced to 15 by applying a reduction algorithm as described in [33]. The difference between the most extreme scenarios in terms of production and demand of energy is about 30%.

Table 3 shows the values imposed for the initial conditions and maximum and minimum storage limits.

Table 3
Limited and initial value imposed.

Battery	
Minimum state-of-charge (SOC_{MIN})	60%
Maximum state-of-charge (SOC_{MAX})	90%
Initial state-of-charge (SOC_{IN})	80%
Maximum charging/discharging power ($P_{B,MAX}$)	18 kW
H2-storage	
Minimum H_2 tank pressure ($p_{H2,MIN}$)	2 bar
Maximum H_2 tank pressure ($p_{H2,MAX}$)	13.8 bar
Initial H_2 tank pressure ($p_{H2,IN}$)	10 bar
Minimum electrolyzer power ($P_{E,MIN}$)	1.5 kW
Maximum electrolyzer power ($P_{E,MAX}$)	6.2 kW
Minimum fuel cell power ($P_{FC,MIN}$)	0.5 kW
Maximum fuel cell power ($P_{FC,MAX}$)	6 kW

The current case study involves 18367 variables of which 12360 binary variables for each scenario tree built at a certain rolling time.

4.2. Results

Starting from the initial conditions, the solver gives the solution of the UC problem, which is the optimal scheduling of the various devices that minimizes total utilization costs. The main output of the program is therefore the on/off status of the various devices. Fig. 6a–d shows the optimal schedules for the electrolyzer and fuel cell for the four weeks studied. As shown in Fig. 6a, the electrolyzer is widely used during the summer week. In this period, a surplus of energy occurs during the central hours of the day mainly due to high PV energy production. The deficit of energy at night is instead supplied by the batteries while the use of the fuel cell is not required.

A less frequent use of the hydrogen storage system occurs during the autumn week (Fig. 6b) and the spring week (Fig. 6d). In these cases, the batteries are mainly used to compensate for the minor difference between energy production and demand, whilst the hydrogen storage system works only for few hours. In contrast, Fig. 6c shows a wide use of the fuel cell during the winter week, when the daily energy produced by the PV and WT power generation plants could only partially cover users' energy demand.

A more accurate simulation model of the system is used to verify the performance of the control system. In these simulation models, implemented in Matlab-Simulink and presented in a previous work [26], the main operating parameters, such as current, voltage, pressure and temperature, are evaluated as the dynamic behavior of each device with a time step of 1 s. Moreover, the verification phase of the EMS was carried out by using actual values for solar radiation and wind speed instead of the corresponding weather forecast.

Fig. 7 shows the power produced by the two RES systems evaluated by using actual data of solar radiation and wind speed. The electrical energy produced during the summer week is 340.0 kW h whereas the overall energy requirement is 268.8 kW h in all cases. A high energy surplus also occurs during the spring week (325.0 kW h of overall energy production). The weekly energy production by RES diminishes in autumn (267.5 kW h) when the difference between energy production and demand is very low. A high energy deficit occurs during the winter week when the weekly energy produced is 243.1 kW h. Fig. 8 shows the charge status of the two storage systems during the periods studied, expressed in terms of SOC of batteries and hydrogen storage level (the latter is the ratio between the current and the maximum hydrogen tank pressure). Since the nominal power output of the PV generator is significantly higher than that of the WT generator, the energy production of the power generation section is greatly affected by the season. In particular, PV production frequently exceeds the energy required by the load during the summer so that large amounts of electrical energy are available for storage. In this situation, high battery SOC values are often reached and therefore the EMS activates the electrolyzer, which operates near its nominal condition. Therefore, the hydrogen produced is stored and subsequently used to produce electricity during periods of great energy deficit as in winter. Unfortunately, the current hydrogen storage capacity of the microgrid is not enough for long-term storage.

A better match between energy production and energy demand occurs during the autumn and spring weeks. In this case, batteries are preferred by the proposed EMS to balance energy production and consumption due to their lower utilization costs compared to the hydrogen storage system.

During the winter, electricity production by RES is usually very low owing to low solar irradiation and operation of the fuel cell is preferred to the batteries to satisfy the large energy deficit in the middle of the day. In this case, the fuel cell can work near its nominal point with high efficiency whereas a decrease in battery efficiency would occur. Therefore, a lower fuel cell utilization cost is obtained while a high battery utilization cost (which linearly depends on the power supplied, as shown by Eq. (13)), is avoided.

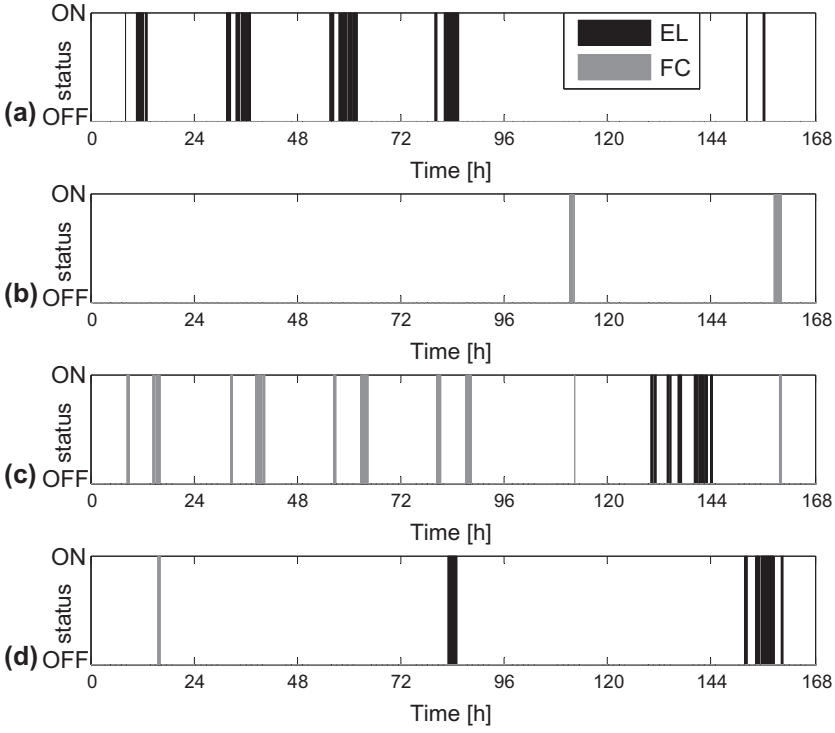

Fig. 6. Generation scheduling of hydrogen storage system for the summer case (a), autumn case (b), winter case (c), spring case (d).

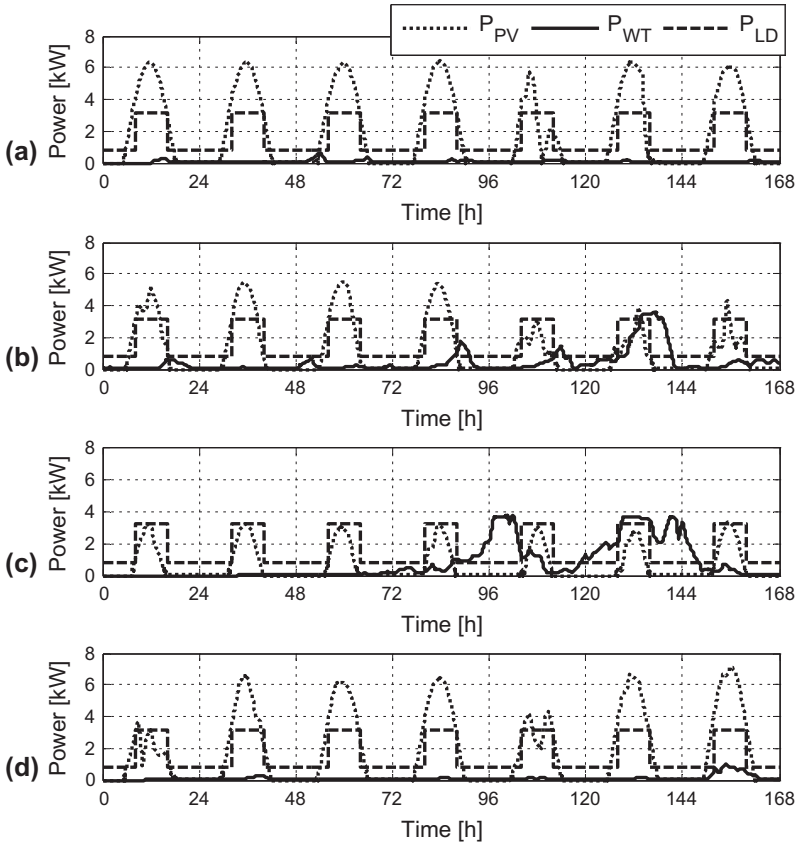

Fig. 7. Power generation and load demand for the summer case (a), autumn case (b), winter case (c) and spring case (d).

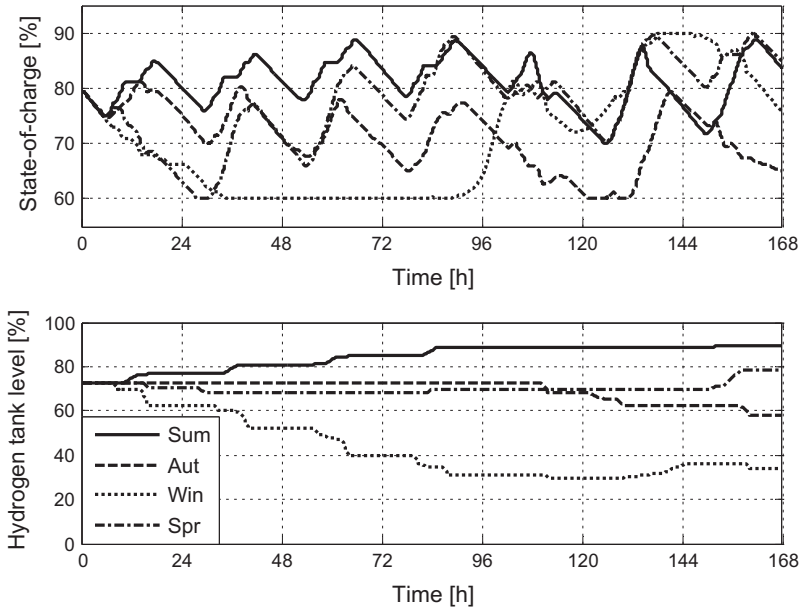

Fig. 8. Time evolution of battery SOC and H_2 tank pressure.

5. EMS comparative analysis

To highlight the capabilities of the proposed EMS, in this section its operational schedules are compared with those of two different EMS: the so-called ''perfect'' EMS and the ''SOC-based'' EMS.

(1) Perfect EMS is based on optimal generation scheduling produced by a perfect forecast of wind speed, solar radiation and energy demand. In this study, perfect EMS is calculated by using real data as input values with only one scenario. Perfect EMS obviously achieves the best results in terms of

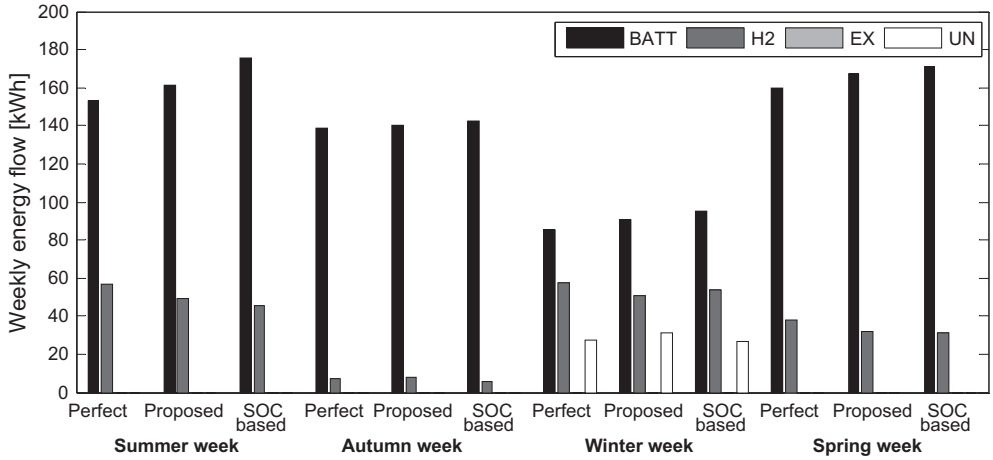

Fig. 9. Weekly energy flows in the two storage system devices.

both minimization of utilization cost and maximization of overall system efficiency. In real applications, load and meteorological data cannot be predicted exactly and perfect EMS is used only as a reference and ideal EMS.

(2) SOC-based EMS is based on optimal generation scheduling produced if the utilization costs of batteries, electrolyzer and fuel cell are neglected. This EMS considers only battery SOC and hydrogen storage level to determine the power flows between the different devices. In particular, when generated power exceeds the power demand and SOC is below 100%, the batteries are charged. When the batteries are fully charged and the excess power is above the electrolyzer minimum operating power, it is activated until the maximum pressure inside the hydrogen tanks is achieved. Vice versa, when generated power is less than the power required by the user, the batteries start to discharge until a minimum value of SOC (SOC_{MIN}) is reached. If the batteries reach the minimum SOC and there is enough hydrogen in the tanks, the fuel cell is turned on. The SOC-based EMS is very simple and suitable for real-time control since it requires very low computational times. However, this EMS is unable to ensure optimal management of the system because it does not take into account costs associated with the on/off status of the devices. Furthermore, the difference in efficiency with which the devices will operate is neglected.

Figs. 9 and 10 and Table 4 summarize the main results in terms of operating hours and utilization costs of the comparative analysis of the three aforementioned EMS.

Results of the proposed EMS should improve with a decrease in rolling time and more frequent meteorological data updating approaching those obtained by the perfect EMS. However, a decrease in the maximum allowable computational time may occur and the EMS may not find the optimal solution in time for every rolling time.

On the other hand, the proposed EMS demonstrates several advantages in comparison to the SOC-based EMS, especially in the summer, winter and spring weeks. Although the total energy exchanged with the hydrogen storage system is almost the same (Fig. 9), a decrease in utilization cost of the hydrogen storage system occurs in the proposed EMS (Fig. 10). Effectively, with this EMS, the hydrogen storage system operates closer to its nominal conditions and therefore closer to its maximum efficiency conditions. In fact, as highlighted in Table 4, an increase in energy conversion efficiency is recorded in the proposed EMS with respect to the SOC-based EMS even though the results obtained with the perfect EMS could not be reached. In addition, an average decrease in the operating cost of about 15% occurs for the proposed EMS compared to the SOC-based EMS. This reduction in operating cost is mainly due to the decrease in the operating hours of the hydrogen storage system.

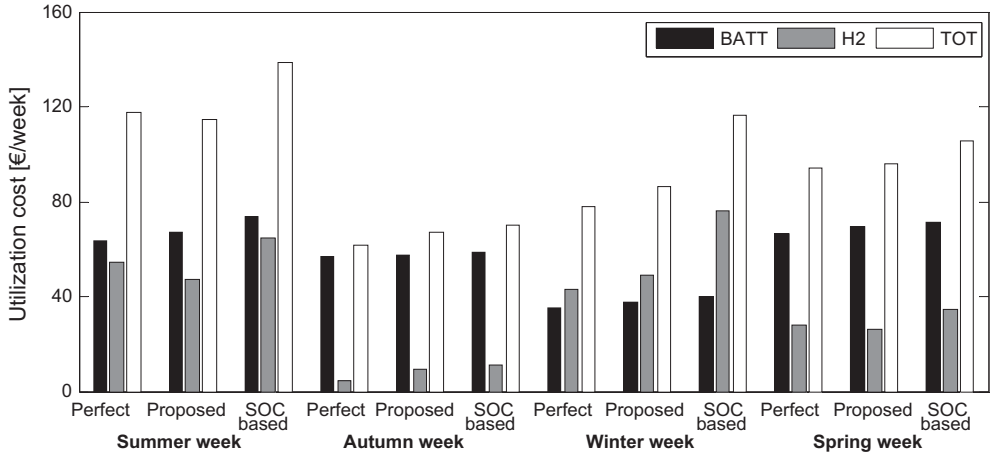

Fig. 10. Weekly utilization costs of storage systems.

Table 4
Summary of results obtained from comparative analysis.

	SOC_{FIN} (%)	$p_{H_2,FIN}$ (bar)	Average η_{H_2} (%)	Average η_{BATT} (%)	Load shedding (kW h)	Operating cost (€/week)
Summer						
Proposed	92.6	13.22	51.2	76.2	–	114.4
Perfect	93.5	13.52	51.4	76.5	–	117.8
SOC-based	83.9	11.75	38.3	75.6	–	138.4
Autumn						
Proposed	65.1	8.03	34.9	77.5	–	66.9
Perfect	82.0	10.32	41.2	77.5	–	61.4
SOC-based	84.4	10.06	32.2	77.4	–	69.8
Winter						
Proposed	75.7	4.69	40.4	77.3	31.4	86.5
Perfect	78.2	3.54	46.3	77.3	27.5	78.1
SOC-based	72.1	2.86	35.8	76.8	26.7	116.1
Spring						
Proposed	84.8	10.85	42.7	87.5	–	96.1
Perfect	80.5	11.20	46.9	87.6	–	94.2
SOC-based	84.8	10.61	37.8	87.4	–	105.8

Finally, Table 4 shows that final values of battery SOC and hydrogen tank pressures are quite similar for the compared EMS. At the end of the summer week, the hydrogen tank pressure increases by more than 3 bar with respect to the initial value (10 bar). This obviously leads to a different initial situation for the following week when the storage tank may be completely filled. Vice versa, the hydrogen tank pressure reaches a lower level at the end of the winter week. This can lead to a significant increase in undelivered power for the following few weeks. Nevertheless, we wish to emphasize that the purpose of this work is to show the benefits and advantages of the proposed EMS instead of analyzing and optimizing the storage capacity of the microgrid studied (the latter will be the task of a following paper).

The main disadvantage of the proposed EMS is the high computational time required to find the optimal solution. The use of linear approximations to avoid nonlinear equations has led to the use of efficient algorithms for linear problems and the certainty of finding the global optimum. On the other hand, it increased the number of constraints and variables and the complexity of the problem. For this case study the problem was solved within 1 h on a 2.57 GHz Core i7 processor. The computation time decreases significantly to about 20 min for the perfect EMS and 5 min for the SOC-based EMS. In all cases, the optimum is found within the available decision time (1 h). Further, more accurate solutions with a better match with the results of the perfect EMS could be achieved by decreasing the rolling time and the update time of the wheatear forecast. However, both operations require major computational resources.

6. Conclusion

In this work, a novel energy management system is proposed for a stand-alone microgrid integrated with an energy storage section based on a battery bank and a hydrogen storage system. Starting from forecasts of weather conditions and load requirements, the proposed EMS calculates the optimal generation scheduling to minimize operating costs and maximize system efficiency. A statistical approach based on the generation of a scenario tree was introduced to account for forecasting uncertainties. To compare the results obtained with the standard EMS widely applied in the literature, a comparative analysis was carried out. In particular, the comparative analysis was carried out with reference to four different climatic situations (a summer week, an autumn week, a winter week and a spring week).

The results show an improvement in system performance compared to the EMS based only on the use of the SOC as a control variable. Furthermore, performance deviated only slightly from that obtained with a perfect EMS, where input data are perfectly forecast. The proposed EMS allows a reduction in operating costs of the energy storage section, especially during the summer and winter weeks. The increase in the time horizon to more than a few weeks and especially the analysis of the annual performance of the microgrid can provide useful information on the optimization of storage capacity.

Acknowledgment

This work was carried out as part of a collaboration agreement with the Sardegna Ricerche Consortium for the management, scientific coordination and development of research activities of the Concentrated Solar Technologies and Hydrogen from RES Laboratory.

Special gratitude to ENEA for the meteorological data provided.

References

[1] World Energy Outlook. Chapter 18, "Measuring progress towards energy for all", International Energy Agency; 2012. p. 529–47.
[2] Yilanci A, Dincer I, Ozturk HK. A review on solar-hydrogen/fuel cell hybrid energy systems for stationary applications. Prog Energy Combust Sci 2009;35:231–44.
[3] Zoulias EI, Glockner R, Lymberopoulos N, Tsoutsos T, Vosseler I, Gavalda O, et al. Integration of hydrogen energy technologies in stand-alone power systems analysis of the current potential for applications. Renew Sustain Energy Rev 2010;10:432–62.
[4] Edwards PP, Kuznetsov VL, David WIF, Brandon NP. Hydrogen and fuel cells: towards a sustainable energy future. Energy Policy 2008;36:4356–62.
[5] Gahleitner G. Hydrogen from renewable electricity: an international review of power-to-gas pilot plants for stationary applications. Int J Hydrogen Energy 2013;38:2039–61.
[6] Bezmalinović D, Barbir F, Tolj I. Techno-economic analysis of PEM fuel cells role in photovoltaic-based systems for the remote base stations. Int J Hydrogen Energy 2013;38:417–25.
[7] Bajpai P, Dash V. Hybrid renewable energy systems for power generation in stand-alone applications: a review. Renew Sustain Energy Rev 2012;16:2926–39.
[8] Ulleberg Ø. The importance of control strategies in PV–hydrogen systems. Sol Energy 2004;76:323–9.
[9] Ipsakis D, Voutetakis S, Seferlis P, Stergiopoulos F, Elmasides C. Power management strategies for a stand-alone power system using renewable energy sources and hydrogen storage. Int J Hydrogen Energy 2009;34:7081–95.
[10] Fernandez LM, Garcia P, Garcia CA, Jurado F. Hybrid electric system based on fuel cell and battery and integrating a single dc/dc converter for a tramway. Energy Convers Manage 2011;52:2183–92.

[11] Dursun E, Kilic O. Comparative evaluation of different power management strategies of a stand-alone PV/Wind/PEMFC hybrid power system. Int J Electr Power Energy Syst 2012;34:81–9.
[12] Dufo-López R, Bernal-Agustín JL, Contreras J. Optimization of control strategies for stand-alone renewable energy systems with hydrogen storage. Renewable Energy 2007;32:1102–26.
[13] Torreglosa JP, García P, Fernández LM, Jurado F. Hierarchical energy management system for stand-alone hybrid system based on generation costs and cascade control. Energy Convers Manage 2014;77:514–26.
[14] Castañeda M, Cano A, Jurado F, Sánchez H, Fernández LM. Sizing optimization, dynamic modeling and energy management strategies of a stand-alone PV/hydrogen/battery-based hybrid system. Int J Hydrogen Energy 2013;38:3830–45.
[15] Ruiz PA, Philbrick CR, Zak E, Cheung KW, Sauer PW. Uncertainty management in the unit commitment problem. IEEE Trans Power Syst 2009;24:642–51.
[16] Logenthiran T, Srinivasan D. Short-term generation scheduling of a microgrid. TENCON 2009–2009 IEEE Region 10 Conference; 2009. p. 1–6.
[17] Zein Alabedinm AM, El-Saadany EF, Salama MMA. Generation scheduling in microgrid under uncertainties in power generation, 2012 IEEE electrical power and energy conference; 2012. p. 133–38.
[18] Tuohy A, Meibom P, Denny E, O'Malley M. Unit commitment for system with significant wind penetration. IEEE Trans Power Syst 2009;24:592–601.
[19] Morais H, Kádár P, Faria P, Vale Zita A, Khodr HM. Optimal scheduling of a renewable micro-grid in an isolated load area using mixed-integer linear programming. Renewable Energy 2010;35:151–6.
[20] Khodr M, El Halabi N, García-Gracia M. Intelligent renewable microgrid scheduling controlled by a virtual power producer: a laboratory experience. Renewable Energy 2012;48:269–75.
[21] Sunpower E18/225-WHT-I solar panel. <http://www.sunpowercorp.com>.
[22] Ropatec Simply Vertical wind turbine. <http://www.ropatec.com/download/IT_dati_tecnici.pdf>.
[23] Ibrahim H, Ilinca A, Perron J. Energy storage systems—characteristics and comparisons. Renew Sustain Energy Rev 2008;12:1221–50.
[24] SMA Sunny Island 5048. <http://www.sma.de/en/products/off-grid-inverters/sunny-island-5048.html>.
[25] Harrison K. Design, integration and control of proton exchange membrane electrolyzer for wind based renewable energy application, Ph.D. thesis, University of North Dakota, USA, August 2006.
[26] Cau G, Cocco D, Petrollese M. Modeling and simulation of an isolated hybrid micro-grid with hydrogen production and storage. Energy Proc 2014;45C:12–21.
[27] Pallottino S, Sechi GM, Zuddas P. A DSS for water resources management under uncertainty by scenario analysis. Environ Model Software 2005;20:1031–42.
[28] Saber AY, Venayagamoorthy GK. Resource scheduling under uncertainty in a smart grid with renewables and plug-in vehicles. IEEE Trans Syst J 2012;26:103–9.
[29] De Boor Carl et al. A practical guide to splines, vol. 27. New York: Springer-Verlag; 1978.
[30] GAMS/Gurobi solver. <www.gurobi.com>.
[31] Italian Air Force weather service. <http://www.meteoam.it/>.
[32] Italian National Agency for New Technologies Energy and Sustainable Economic Development (ENEA), Italian Solar Radiation Atlas, <http://www.solaritaly.enea.it/Previsioni/Previsioni-dettagliEn-casaccia.php>.
[33] GAMS SCENRED, <www.gams.com/dd/docs/solvers/scenred.pdf>.
[34] Cau G, Cocco D, Petrollese M, Tola V. Assessment of a hybrid stand-alone power system with hydrogen production and storage. In: Proc. 3rd International conference on microgeneration and related technologies; 2013.